

## A New Phase Shifted Converter using Soft Switching Feature for Low Power Applications

Aswathi M. Nair<sup>1</sup>, K. Keerthana<sup>2</sup>

<sup>1,2</sup> (P.G (PE&D) student, Asst. Professor, Department of EEE, Dhanalakshmi Srinivasan Engineering College, Perambalur-12)

**Abstract:** This project presents a new dual bridge DC/DC converter for Low power applications which can solve the drawbacks of conventionally existing phase-shifted full bridge converters. It eliminates the narrow zero voltage switching (ZVS) range. The proposed converter configuration is composed of leading leg and lagging leg SHBIs. Phase shift control is employed to control the phase difference between the two bridge inverters. By shifting the phase, the converter changes the two inverters output voltage overlapping area to regulate its output voltage. At the secondary side, a centre tapped rectifier with two low current ratings are used. This structure allows the proposed converter to have the advantages of full ZVS range. ZVS eliminates turn on switching loss of the power switch. In this paper, the circuit analysis, operating principle and relevant analysis results of the proposed converters are presented.

**Index terms:** Full bridge converter, phase shift control, zero voltage switching.

### I. Introduction

DC voltage power supplies are utilized in most electrical/electronic equipment in order to meet the power requirement of the electronic circuits in the equipment. At higher power, voltage, or current ratings more complex power converters become necessary. When galvanic isolation or a significant voltage/current level change is required, these converters are accompanied with an isolation transformer. However, the converter suffers from an increased loss in the duty cycle, and a severe reverse-recovery phenomenon is generated on the additional clamping diodes when there is a light load [1], [2]. In addition, the small duty cycle has detrimental effects on converter performance, such as a large ripple current through the output inductor LO [3] and the ZVS range of lagging-leg switches is very narrow under load variation. For this reason, its conversion efficiency is severely degraded as the load decreases [4]. PSFB converters extending the ZVS range without the increase of duty-cycle loss were introduced in [6]–[9]. In the converters, however, the current stress of all the switches is higher than the traditional PSFB converter due to the assistant current source for a wide ZVS range, which leads to the increase in conduction loss. To minimize the increase of current stress, one or two bulky inductors and some coupled inductors with large inductance are additionally required. The PSFB converters with a current-doubler rectifier can also solve the problems. However, the current ripple of two output inductors must be designed to be very large for a wide ZVS range. This results in an increase of RMS current stress in the converters [10], [11]. In [12] and [13], the PSFB converters with two transformers were introduced. Due to the use of two transformers, the ZVS operation in the converters is achieved under entire load conditions. However, the dc bias currents equal to half the primary-reflected load current, which flows through the transformers, reduce the utilization of the transformers. The PSFB converters with ZVS and zero-current-switching (ZCS) operation can provide another solution to the problems. In these converters, leading-leg switches are turned ON with ZVS and lagging-leg switches are turned OFF with ZCS. Thus, MOSFETs as leading-leg switches and IGBTs as lagging-leg switches are generally employed. Because the ZVS operation of leading-leg switches is achieved by the same way as that of the traditional PSFB converter, its range is wide under load variation. Moreover, nearly constant efficiency can be obtained over a wide input voltage range because there is no circulating current in the converters. However, for ZCS operation and countermeasures to side effects such as high secondary-voltage stress and primary-current overshoot, they require many additional components, which results in high cost and a complex structure [14]–[17]. In addition, using IGBTs to suit ZCS operation precludes the use of high switching frequency to realize smaller magnetic components and capacitors [18]–[19].

The objective is to develop a soft switching converter that achieves zero voltage switching over a widely varying load for low power applications. In this paper a new soft-switching dc/dc converter with a full ZVS range for high voltage applications is developed. It is composed of two symmetric half bridge inverters (leading leg and lagging leg SHBIs, which are placed in parallel on the primary side and are driven in a phase shifting manner to regulate the output voltage. This structure allows that the proposed converter has

the following advantages that All the switches is turned ON with ZVS under entire load conditions without any additional large resonant inductors or circuits, while the conduction loss caused by the assistant current source extending the ZVS range is minimized due to its reduced conduction path.

## II. Proposed Converter Configuration

In order to overcome the problems of the traditional PSFB converter, many studies have been conducted. First, to remove the circulating current and reduce the large output inductor, the frequency modulated FB converter was developed. The operating range of its switching frequency, however, is very widely changed in a wide input voltage range, which leads that it is difficult to design optimally the magnetic components and capacitors. In addition, the converter cannot achieve ZVS in a wide range of load variation. The ZVS range of lagging leg switches in the traditional PSFB converter can be extended by making the leakage inductance of the transformer very large and/or adding an external resonant inductor with large inductance. However, this approach increases duty cycle loss, which results in high secondary voltage stress and primary conduction losses. Another PSFB converter uses a resonant inductor to extend the ZVS range of lagging leg switches and needs two clamping diodes for easy reduction of the secondary voltage overshoot and oscillation, However converter suffers from increased duty cycle loss.

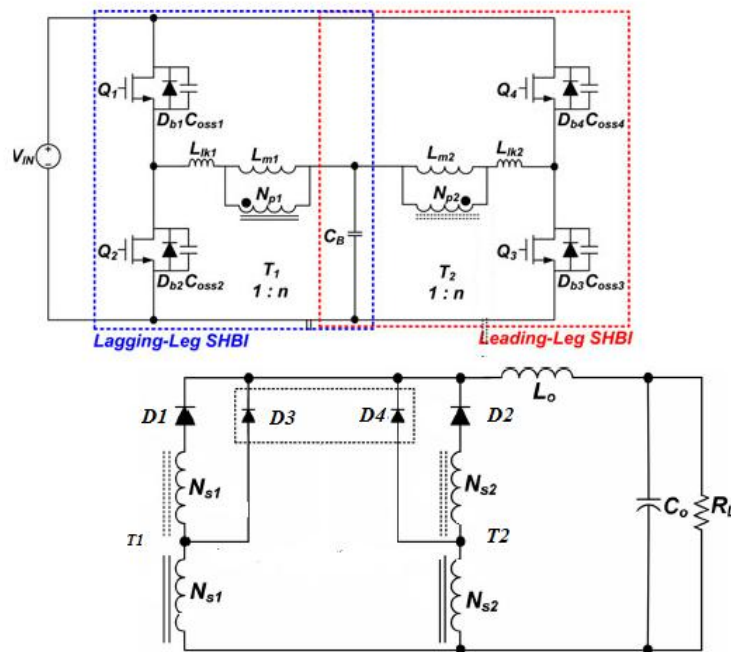


Fig.2.Proposed converter

The proposed system presents a new soft switching dc/dc converter with a full ZVS range for medium voltage applications is proposed. The proposed converter is composed of two symmetric half bridge inverters (TSHBIs), leading leg and lagging leg SHBIs, which are placed in parallel on the primary side and are driven in a phase-shifting manner to regulate the output voltage

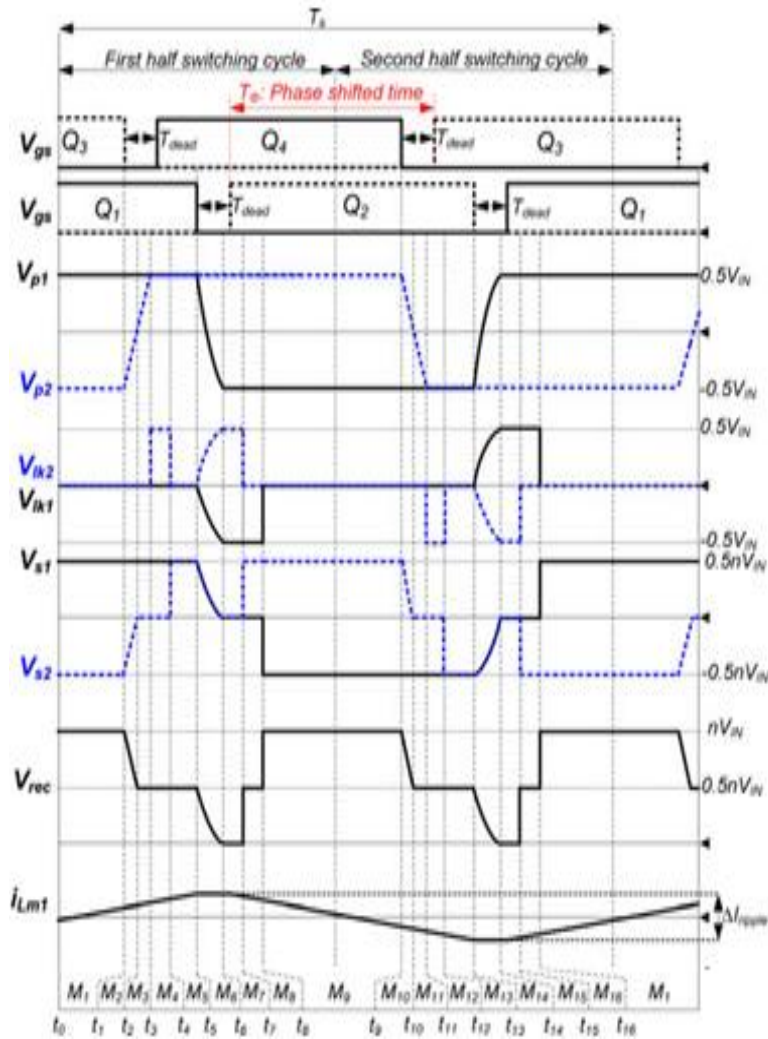


Fig.3.Operating waveforms

### III. Principle of Operation

The circuit diagram of the proposed converter is shown in Fig.2. The primary side consists of four switches and two transformers transferring the input power to the secondary side alternately. Fig. 3 shows the operating waveforms of the proposed converter in the steady state,

**Mode 1[t<sub>0</sub>-t<sub>1</sub>]:** Mode 1 begins when switches Q<sub>1</sub> and Q<sub>3</sub> are in on-state and diodes D<sub>1</sub> and D<sub>3</sub> are conducting. During this mode, the primary voltages V<sub>p1</sub>(t) and V<sub>p2</sub>(t) of the transformers T<sub>1</sub> and T<sub>2</sub> are the positive and negative halves of the input voltage, respectively. Thus, the magnetizing current i<sub>Lm1</sub>(t) increases linearly from its initial value. However, i<sub>Lm2</sub>(t) is nearly zero because the magnetizing inductance L<sub>m2</sub> of T<sub>2</sub> is very large. The secondary voltages V<sub>s1</sub>(t) and V<sub>s2</sub>(t) of T<sub>1</sub> and T<sub>2</sub> are the positive and negative halves of the input voltage reflected to the secondary by the turns ratio n, respectively, thus the power is transferred from the input to the output through T<sub>1</sub>, T<sub>2</sub>, D<sub>1</sub>, and D<sub>3</sub>. The output voltage of rectifier V<sub>rec</sub>(t) becomes nV<sub>IN</sub>, which is the sum of V<sub>s1</sub>(t) and -V<sub>s2</sub>(t). The primary currents in this mode can be expressed as follows:

$$\begin{aligned} i_{p1}(t) &= i_{Lm1}(t) + ni_{sec1}(t) = i_{Lm1}(t) + ni_{D1}(t) \\ &= i_{Lm1}(t) + nI_o \end{aligned}$$

$$i_{p1}(t) = i_{Lm2}(t) + ni_{sec2}(t) \approx ni_{sec2}(t) = -ni_{D3}(t) = -nI_o \quad (1)$$

**Mode 2[t<sub>1</sub>-t<sub>2</sub>]:** Mode 2 begins when Q<sub>3</sub> is turned OFF at t<sub>1</sub>. Then, the voltage across C<sub>oss3</sub> is charged linearly and the voltage across C<sub>oss4</sub> is discharged linearly by the energy stored in the output inductor L<sub>o</sub>. V<sub>p2</sub>(t) increases from -0.5V<sub>IN</sub> to zero and V<sub>p1</sub>(t) is continuously maintained at 0.5V<sub>IN</sub>, which

increases continuously  $i_{L_{m1}}(t)$ .  $V_{s2}(t)$  also increases from  $-0.5nV_{IN}$  to zero and  $V_{s1}(t)$  becomes  $0.5nV_{IN}$ . Thus,  $V_{rec}(t)$  falls from  $nV_{IN}$  to  $0.5nV_{IN}$ . The expressions of primary currents in this mode are the same as in mode 1. The voltages can be expressed as follows:

$$\begin{aligned} V_{Q3}(t) &= nI_o \frac{(t-t_1)}{2C_{oss}}, V_{Q4}(t) = V_{IN} - V_{Q3}(t) \\ V_{p2}(t) &= -0.5V_{IN} + nI_o \frac{(t-t_1)}{2C_{oss}} \\ V_{rec}(t) &= V_{s1}(t) + V_{s2}(t) = nV_{IN} - \frac{n^2I_o}{2C_{oss}}(t-t_1) \end{aligned} \quad (2)$$

**Mode 3[t<sub>2</sub>-t<sub>3</sub>]:** Mode 3 begins when  $V_{p2}(t)$  becomes zero in mode 2. At the same time,  $V_{s2}(t)$  becomes zero and the voltage across  $C_{oss3}$  or  $C_{oss4}$  is continuously charged or discharged by the resonance, respectively.  $V_{p2}(t)$  increases from zero to  $0.5V_{IN}$  with a sinusoidal waveform and  $V_{p1}(t)$  is continuously maintained at  $0.5V_{IN}$ . The voltages and currents in this mode are given by

$$\begin{aligned} V_{p1}(t) &= 0.5V_{IN}, V_{s1}(t)=0.5nV_{IN}, V_{s2}(t)=0 \\ V_{rec}(t) &= 0.5nV_{IN}, V_{p2}(t)=nI_{oz01}\sin\omega_{o1}(t-t_2) \\ V_{Q3}(t) &= 0.5V_{IN} + nI_{oz01}\sin\omega_{o1}(t-t_2) \\ V_{Q4}(t) &= V_{IN} - V_{Q3}(t), i_{p1}(t) = i_{p2}(t_2) + 0.5V_{IN} \frac{(t-t_2)}{L_{m1}} \\ i_{p2}(t) &= -nI_o \cos\omega_{o1}(t-t_2) \end{aligned}$$

where

$$\omega_{o1} = \frac{1}{\sqrt{2L_{lk2}C_{oss}}}, z_{o1} = \frac{\sqrt{L_{lk2}}}{\sqrt{2C_{oss}}} \quad (3)$$

**Mode 4[t<sub>3</sub>-t<sub>4</sub>]:** Mode 4 begins when  $V_{p2}(t)$  reaches  $0.5V_{IN}$  in mode 3. Then, the parasitic diode  $D_{b4}$  of  $Q_4$  starts to conduct and  $Q_4$  is turned ON with ZVS. During this mode,  $V_{s2}(t)$  is maintained at zero, thus the voltage  $0.5V_{IN}$  appears on the leakage inductor  $L_{lk2}$ . Due to this voltage across  $L_{lk2}$ , the commutation of  $D_3$  is progressed.  $V_{p1}(t)$  and  $V_{rec}(t)$  are continuously maintained at  $0.5V_{IN}$  and  $0.5nV_{IN}$ , respectively. During this mode, the power is transferred from the input to the output through  $T_1, T_2, D_1$  and  $D_3$ . The currents in this mode can be expressed as follows:

$$\begin{aligned} i_{p1}(t) &= i_{p1}(t_3) + 0.5V_{IN} \frac{(t-t_3)}{L_{m1}} \\ i_{p2}(t) &= -nI_o + 0.5V_{IN} \frac{(t-t_3)}{L_{lk2}}, i_{D1}(t) = I_o \\ i_{D3}(t) &= I_o \end{aligned} \quad (4)$$

**Mode 5[t<sub>4</sub>-t<sub>5</sub>]:** Mode 5 begins when the commutation of  $D_3$  is completed at  $t_4$  and only  $D_1$  conducts. In this mode, the primary current  $i_{p2}(t)$  [or the secondary current  $i_{sec2}(t)$ ] in leading-leg SHBI is zero, i.e., the power is transferred from the input to the output through only  $T_1$  and  $D_1$ . During this mode, the voltages and currents are given by

$$\begin{aligned} V_{p1}(t) &= V_{p2}(t) = 0.5V_{IN}, V_{s1}(t) = V_{s2}(t) = 0.5nV_{IN}, \\ V_{rec}(t) &= 0.5nV_{IN}, i_{p1}(t) = i_{p1}(t_4) + 0.5V_{IN} \frac{(t-t_4)}{L_{m1}} \\ i_{p2}(t) &= i_{sec2}(t) = 0 \end{aligned} \quad (5)$$

**Mode 6[t<sub>5</sub>-t<sub>6</sub>]:** Mode 6 begins when  $Q_1$  is turned OFF at  $t_5$ . At the same time, diode  $D_4$  starts to conduct. Then, the resonance of  $C_{oss1}, C_{oss2}, L_{lk1}$ , and  $L_{lk2}$  occurs in the primary power path. The voltage across  $C_{oss1}$  or  $C_{oss2}$  is discharged or charged by the resonance, respectively.  $V_{p1}(t)$  is decreased from  $0.5V_{IN}$  to  $-0.5nV_{IN}$  and  $V_{rec}(t)$  falls to zero. The commutation between  $D_1$  and  $D_4$  is also progressed. The voltages and currents in this mode can be expressed as follows:

$$\begin{aligned} V_{Q1}(t) &= V_{IN} - V_{Q2}(t) \\ V_{Q2}(t) &= V_{IN} - z_{o2} i_{p1}(t_5) \sin\omega_{o2}(t-t_5) \\ V_{p1}(t) &= 0.5V_{IN} - z_{o2} i_{p1}(t_5) \sin\omega_{o2}(t-t_5) \\ V_{p2}(t) &= 0.5V_{IN} \\ V_{s1}(t) &= V_{s2}(t) = V_{rec}(t) \end{aligned}$$

$$\begin{aligned}
 &= 0.5nV_{IN} - n\omega_{o2}L_{lk2}i_{p1}(t_5) \sin \omega_{o2}(t - t_5) \\
 i_{p1}(t) &= i_{p1}(t_5) \cos \omega_{o2}(t - t_5) \\
 i_{p2}(t) &= (nI_o + 0.5\Delta I_{ripple}) - i_{p1}(t_5) \cos \omega_{o2}(t - t_5) \\
 i_{D4}(t) &= I_o - i_{D1}(t) = i_{p2}(t)/n
 \end{aligned}$$

where

$$i_{p1}(t_5) = nI_o = 0.5\Delta I_{ripple}, \quad \Delta I_{ripple} = \frac{V_{IN}T_s}{4L_{m1}}$$

$$\omega_{o2} = \frac{1}{\sqrt{2(L_{lk1}+L_{lk2})C_{oss}}}, \quad z_{o2} = \frac{\sqrt{L_{lk1}+L_{lk2}}}{\sqrt{2C_{oss}}} \quad (6)$$

**Mode 7[t<sub>6</sub>-t<sub>7</sub>]:** Mode 7 begins when  $V_{p1}(t)$  reaches  $-0.5V_{IN}$  in mode 6. Then, the parasitic diode  $D_{b2}$  of  $Q_2$  starts to conduct and  $Q_2$  is turned ON with ZVS. In this mode, all the secondary voltages of the transformers,  $V_{sec1}(t)$  and  $V_{sec2}(t)$ , are zero, thus  $V_{rec}(t)$  becomes zero. Due to  $V_{rec}(t)=0$ , the load power is supplied from the energy stored in the output inductor  $L_o$  at  $t_6$ . Because  $V_{p1}(t)=-0.5V_{IN}$ ,  $V_{p2}(t)=0.5V_{IN}$ , and  $V_{s1}(t) = V_{s2}(t) = 0$  during this mode, the voltage  $V_{lk1}(t)$  across  $L_{lk1}$  equals to  $-0.5V_{IN}$  and the voltage  $V_{lk2}(t)$  across  $L_{lk2}$  equals to  $0.5V_{IN}$ . Due to these leakage inductors' voltages,  $i_{p1}(t)$  or  $i_{D1}(t)$  decreases linearly and  $i_{p2}(t)$  or  $i_{D4}(t)$  increases linearly. The currents can be expressed as follows:

$$\begin{aligned}
 i_{p1}(t) &= i_{p1}(t_6) - \frac{0.5V_{IN}}{L_{lk1}}(t-t_6) \\
 i_{p2}(t) &= i_{p2}(t_6) + \frac{0.5V_{IN}}{L_{lk2}}(t-t_6) \\
 i_{D4}(t) &= I_o - i_{D1}(t) = i_{p2}(t)/n
 \end{aligned} \quad (7)$$

**Mode 8[t<sub>7</sub>-t<sub>8</sub>]:** Mode 8 begins when the current through  $D_4$ ,  $i_{D4}(t)$ , reaches the output current  $I_o$  and  $D_1$  is naturally turned OFF. At the same time,  $V_{s1}(t)$  becomes zero and  $V_{s2}(t)$  becomes  $0.5nV_{IN}$ . Thus, during this mode, the voltage  $0.5V_{IN}$  appears on  $L_{lk1}$ , and the commutation of  $D_2$  starts.  $V_{rec}(t)$  equals to  $0.5nV_{IN}$ . The currents in this mode can be expressed as follows:

$$\begin{aligned}
 i_{p1}(t) &= i_{p1}(t_7) - \frac{0.5V_{IN}}{L_{lk1}}(t-t_7), \quad i_{p2}(t) = nI_o \\
 i_{D4}(t) &= I_o, \quad i_{D2}(t) = I_o = \frac{0.5V_{IN}}{nL_{lk1}}(t-t_7)
 \end{aligned} \quad (8)$$

At the end of this mode,  $i_{D2}(t)$  reaches the output current  $I_o$ . Then, the power is transferred from the input to the output through  $T_1$ ,  $T_2$ ,  $D_2$ , and  $D_4$ .

**Mode 9-16[t<sub>8</sub>-t<sub>16</sub>]:** The operations from mode 9 to mode 16 are the same as previous modes except for the direction of powering path.

#### IV. Experimental Results

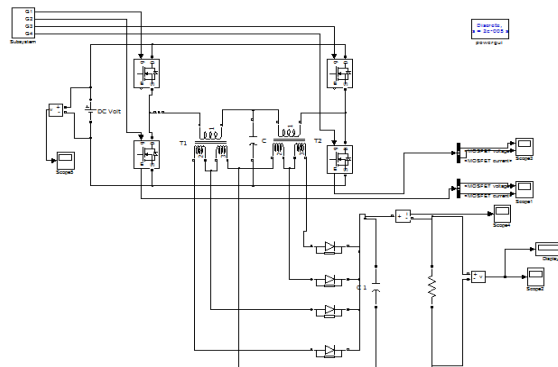


Fig.4.Simulation Circuit

Digital simulation is done using MATLAB and the results are presented here. Open loop system of 200V/48V, 100 KHz dc/dc converter is shown in Fig.4. Input voltage of 200V is shown in

Fig.5. The output voltage in open loop system is shown in Fig.8.. The output current is shown in fig.9. The output voltage increases with the increase in the input voltage. Figs.6. and 7 shows the ZVS waveforms of the leading-leg or lagging-leg SHBIs. From Figs. 6 and 7, it is clear that all the switches in the proposed converter are turned ON with ZVS under entire load conditions.

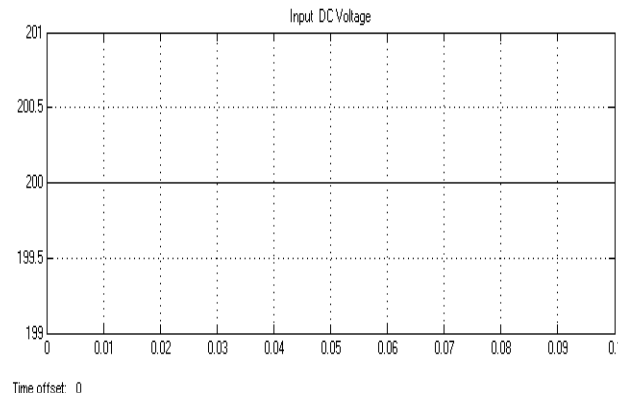


Fig.5.Input DC voltage

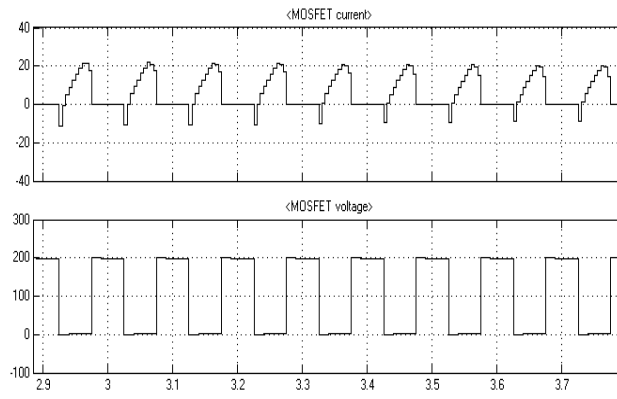


Fig.6.Waveform indicating ZVS condition of the lagging-leg switch  $Q_2$

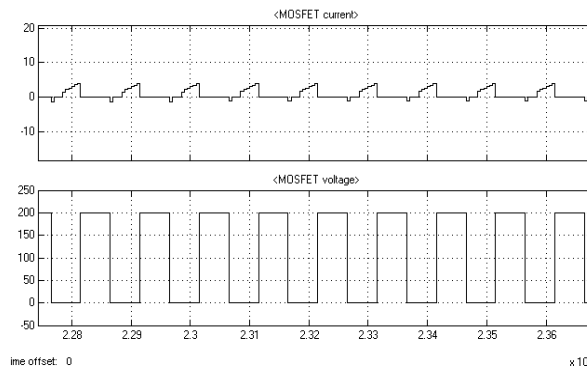


Fig.7.Waveform indicating ZVS condition of the leading-leg switch  $Q_3$

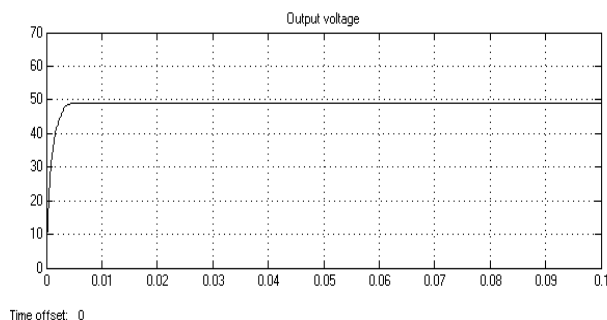


Fig.8.Converter output voltage

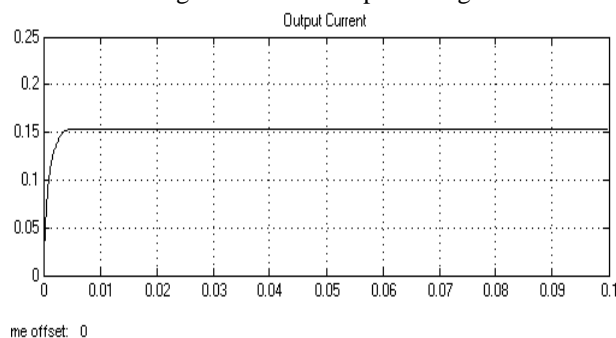


Fig.9.Converter output current

## VI. Conclusion

In this paper a new soft-switching dc/dc converter with a full ZVS range for low voltage applications is developed. It is composed of two symmetric half bridge inverters (leading leg and lagging leg SHBIs, which are placed in parallel on the primary side and are driven in a phase shifting manner to regulate the output voltage. With an auxiliary centre tapped rectifier at the secondary side with two low current rating diodes, Zero voltage switching of the switches are achieved. This DC/DC converter is relatively suitable for low power applications. Moreover, the proposed converter can be integrated with other to achieve soft-switching feature. A prototype has been designed to prove the validity of the proposed converter. The proposed converter is suitable for the server and telecommunication equipments using 48 V bus voltage, and requiring the high efficiency and high power density. Also, in the near future, it is suitable for the new automotive 48 V power systems.

## REFERENCES

- [1] W. Chen, X. Ruan, and R. Zhang, "A novel zero-voltage-switching PWM full bridge converter," *IEEE Trans. Power Electron.*, vol. 23, no. 2, pp. 793–801, Mar. 2008.
- [2] W. Chen, X. Ruan, Q. Chen, and J. Ge, "Zero-voltage-switching PWM full-bridge converter employing auxiliary transformer to reset the clamping diode current," *IEEE Trans. Power Electron.*, vol. 25, no. 5, pp. 1149–1162, May 2010.
- [3] Y. Shin, C. Kim, and S. Han, "A pulse frequency modulated full bridge DC/DC converter with series boost capacitor," *IEEE Trans. Ind. Electron.*, vol. 58, no. 11, pp. 5154–5162, Nov. 2011.
- [4] B. Chen and Y. Lai, "Switching control technique of phase-shiftcontrolled full-bridge converter to improve efficiency under light-load and standby conditions without additional auxiliary components," *IEEE Trans. Power Electron.*, vol. 25, no. 4, pp. 1001–1011, Apr. 2010.
- [5] X. Cho, K. Cho, and G. Moon, "A new phase-shifted full-bridge converter with maximum duty operation for server power system," *IEEE Trans. Power Electron.*, vol. 26, no. 12, pp. 3491–3500, Dec. 2011.
- [6] Wu, J. Zhang, and Z. Qian, "Analysis and optimal design considerations for an improved full bridge ZVS DC-DC converter with high efficiency," *IEEE Trans. Power Electron.*, vol. 21, no. 5, pp. 1225–1234, Sep. 2006.
- [7] M. Borage, S. Tiwari, S. Bhardwaj, and S. Kotaiah, "A full-bridge DCDC converter with zero-voltage-switching over the entire conversion range," *IEEE Trans. Power Electron.*, vol. 23, no. 4, pp. 1743–1750, Jul. 2008.
- [8] M. Borage, S. Tiwari, and S. Kotaiah, "A passive auxiliary circuit achieves zero-voltage-switching in full-bridge converter over entire conversion range," *IEEE Trans. Power Electron.*, vol. 3, no. 3, pp. 141–143, Dec. 2005.
- [9] Y. Jang, M. M. Jovanović, and Y. Chang, "A new ZVS-PWM full-bridge converter," *IEEE Trans. Power Electron.*, vol. 18, no. 5, pp. 1122–1129, Sep. 2003.
- [10] T. Wu, C. Tsai, Y. Chang, and Y. Chen, "Analysis and implementation of an improved current-doubler rectifier with coupled inductors," *IEEE Trans. Power Electron.*, vol. 23, no. 6, pp. 2681–2693, Nov. 2008.

- [11] N. H. Kutkut, D. M. Divan, and R. W. Gascoigne, "An improved full-bridge zero-voltage-switching PWM converter using a two-inductor rectifier," *IEEE Trans. Ind. Appl.*, vol. 31, no. 1, pp. 119–126, Jan. 1995.
- [12] G. Koo, G. Moon, and M. Youn, "Analysis and design of phase shift full bridge converter with series-connected two transformers," *IEEE Trans. Power Electron.*, vol. 19, no. 2, pp. 411–419, Mar. 2004.
- [13] H. Yoon, S. Han, E. Choi, G. Moon, and M. Youn, "Zero-voltage switching and soft-commutation two-transformer full-bridge PWM Converter using the voltage-ripple," *IEEE Trans. Ind. Electron.*, vol. 55, no. 3, pp. 1478–1488, Mar. 2008.
- [14] X. Wu, X. Xie, J. Zhang, R. Zhao, and Z. Qian, "Soft switched full bridge DC-DC converter with reduced circulating loss and filter requirement," *IEEE Trans. Power Electron.*, vol. 22, no. 5, pp. 1949–1955, Sep. 2007
- [15] X. Wu, X. Xie, C. Zhao, Z. Qian, and R. Zhao, "Low voltage and current stress ZVZCS full bridge DC-DC converter using center tapped rectifier reset," *IEEE Trans. Ind. Electron.*, vol. 55, no. 3, pp. 1470–1477, Mar. 2008.
- [16] K. Seok and B. Kwon, "An improved zero-voltage and zero-currentswitching full-bridge PWM converter using a simple resonant circuit," *IEEE Trans. Ind. Electron.*, vol. 48, no. 6, pp. 1205–1209, Dec. 2001.
- [17] J. Dudrik and N. Trip, "Soft-switching PS-PWM DC-DC converter for full-load range applications," *IEEE Trans. Ind. Electron.*, vol. 57, no. 8, pp. 2807–2814, Aug. 2010.
- [18] T. T. Song and N. Huang, "A novel zero-voltage and zero-currentswitching full-bridge PWM converter," *IEEE Trans. Power Electron.*, vol. 20, no. 2, pp. 286–291, Mar. 2005
- [19] E. Kim and Y. Kim, "A ZVZCS PWM FB DC/DC converter using a modified energy-recovery snubber," *IEEE Trans. Ind. Electron.*, vol. 49, no. 5, pp. 1120–1127, Oct. 2002.